

## The influence of CuO nanoparticles and boron wastes on the properties of cement mortar

M. Yildirim, E.M. Derun✉

Department of Chemical Engineering, Faculty of Chemical and Metallurgical Engineering, Yildiz Technical University (Istanbul, Turkey)  
✉moroydor@gmail.com, moroydor@yildiz.edu.tr

Received 31 March 2017  
Accepted 7 November 2017  
On line first 13 July 2018

**ABSTRACT:** In this study, compressive and flexural strength, thermal properties, and pore structure of mortars modified with two types of boron waste and different amounts of CuO nanoparticles were investigated. The binders were prepared with 3% of borogypsum or borax waste and nano-CuO at concentration up to 4%. The setting time, compressive and flexural strength at 3, 7, and 28 days, DTA/TG, XRD, BET, and water absorption tests were carried out, and optimal nano-CuO percentages were determined. It was observed that nano-CuO addition in the range 2%–2.5% can improve mechanical properties, reduce the amount of unreacted portlandite, increase water absorption resistance, and decrease the setting time for borogypsum-containing mortars. The optimum nano-CuO replacement ratio changes between 0.5%–1% for borax waste-containing mortars. The results showed that nano-CuO was able to promote hydration reactions, act as a nanofiller, and provide a kernel for nucleation reactions.

**KEYWORDS:** Compressive strength; Mortar; Thermal analysis; Waste treatment; X-ray diffraction.

**Citation/Citar como:** Yildirim, M.; Derun, E.M. (2018) The influence of CuO nanoparticles and boron wastes on the properties of cement mortar. *Mater. Construcc.* 68 [331], e161 <https://doi.org/10.3989/mc.2018.03617>

**RESUMEN:** *Influencia de las nanopartículas de CuO y los residuos de boro en las propiedades de morteros de cemento.* En este estudio, se investigaron las resistencias a compresión y flexión, las propiedades térmicas y las estructuras porosas de morteros modificados con dos tipos de residuos de boro y distintas cantidades de nanopartículas de CuO. Los morteros se prepararon con un 3 % de boro-yeso o residuos de boro y nano-CuO, en concentraciones de hasta el 4 %. Se realizaron ensayos de tiempo de fraguado, resistencias mecánicas a 3, 7 y 28 días, ATD/TG, DRX, área BET y absorción de agua y se determinaron los porcentajes óptimos de nano-CuO. Se observó que la adición de nano-CuO en el rango del 2–2,5 % mejora las propiedades mecánicas, reduce la cantidad de portlandita sin reaccionar, aumenta la resistencia de absorción del agua y disminuye el tiempo de fraguado en morteros que contienen residuos de boro. Los resultados muestran que el nano-CuO favorece las reacciones de hidratación, actúa como nanofiller y proporciona un punto para las reacciones de nucleación.

**PALABRAS CLAVE:** Resistencias a compresión; Mortero; Análisis térmico; Tratamiento de residuos; Difracción de rayos X.

**ORCID ID:** M. Yildirim (<http://orcid.org/0000-0003-1383-3151>); E. M. Derun (<http://orcid.org/0000-0002-8587-2013>)

**Copyright:** © 2018 CSIC. This is an open-access article distributed under the terms of the Creative Commons Attribution 4.0 International (CC BY 4.0) License.

## 1. INTRODUCTION

The use of industrial wastes as supplementary cementitious materials (SCMs) instead of cement, thereby eliminating 5% of the world's carbon dioxide emissions, has grown in the last decades in line with sustainable and environmentally friendly production approaches. Researchers have approached the problem of improving properties to cement composites by using different SCMs, including fly ash, granulated blast furnace slag, rice husk ash, and silica fume (1). Also, waste formed during production of borate chemicals (boric acid and tincalconite) have been utilized in construction applications because of their gypsum-like composition and pozzolanic properties (2–4). The wide range of use of boron minerals brings higher production capacities, which has resulted in more than 900.000 tons of boron derivative waste in Turkey alone (5). The study carried out by Targan et al. showed usage boron waste with natural pozzolans improves the bending strength of specimens (2). Olgun et al. mentioned that boron waste can increase the long term mechanical properties of mortars (3). However, Topcu and Boga showed that boron waste improves the durability, but decreases the mechanical properties (4). Also, literature studies proved boron waste has the set retarding effects (6).

Nanotechnology is an attractive research area with many applications because of the advantages of nanoscale (1–100 nm) materials. Nanoparticles, including nano-silica, nano-alumina, nano-titania, and nano-copper oxide, are used in cement composites to enhance mechanical and physical durability and chemical stability. Nanoparticles can be divided into two groups: nanoparticles that show pozzolanic activity such as nano-silica and nano-alumina, and those used as nanofillers and nano-nuclei such as nano-titania, nano-copper oxide, and nano-zinc oxide (7–16).

When nanoparticles disperse uniformly in the cement matrix, they produce a larger available surface area for hydration reactions. At early stages of hydration, nanoparticles act as a kernel, and hydration products envelop them tightly, resulting in a more compact, denser cement matrix. The generation of heterogeneous nucleation sites by nanoparticles promotes the formation of hydration products and limits the amount of  $\text{Ca}(\text{OH})_2$ . That results in improvement of the strength and durability of cement composites and reduced permeability through densification of the microstructures (17–22).

Many researchers have investigated the effects of nanoparticles on the mechanical and physical properties of cement composites. However, most of the studies have been concerned with application of silica, alumina, titania and iron oxide nanoparticles. Because of their pozzolanic effects

nano-silica and nano-alumina are the most popular nanoparticles in the research. Li et al. reinforced cement composite with nano-alumina and revealed that the compressive strength and elastic modulus of mortars were improved by incorporating nano-alumina into matrix (18). Sneff et al. showed nano-silica modified the fresh properties of cement mortars and decreased the setting time of mortars up to 60% (9). Qing et al. revealed that nano-silica accelerated the hydration process and using nano-silica up to 5% increased the mechanical properties of cement composites. The pozzolanic reaction of nano-silica with  $\text{Ca}(\text{OH})_2$  may be as follows (17) [Eq. 1, 2 and 3].



However, some studies have observed the influence of nano copper oxide on fresh and hardening features of cement-based materials. Nazari and Riahi (21, 22) investigated the mechanical and thermal properties of self-compacting concrete with different amounts of CuO nanoparticles added, and their experimental results showed that increasing the proportion of CuO nanoparticles up to 4% could improve properties of the concrete. In another stud, in which CuO was used together with ground granulated blast furnace slag, Nazari et al. (22) found that replacing the cement up to 3% by CuO nanoparticles could accelerate formation of calcium silicate hydrates (C-S-H) and reduce water permeability. Miyandehi et al. studied the combined effects of CuO nanoparticles and rice husk ash on the durability, strength, and permeability of cement mortars; their results showed that CuO nanoparticles reduced the porosity of the cement matrix and increased both the compressive strength and durability of mortar specimens (23).

Although there are studies incorporating CuO nanoparticles with cement composites, no study to date has examined the binary effects of boron waste and CuO nanoparticles on the fresh and hardened properties of cement mortar. The present study investigated the effects of boron waste and various amounts of CuO nanoparticles on the mechanical and thermal properties and the pore structure of cement mortars, evaluating both their compressive and flexural strength. Thermogravimetric analysis was used to evaluate the thermal properties, and the properties of the pore structure of mortars were determined by the Brunauer-Emmett-Teller (BET) method and water absorption test. The phase composition of mortars was determined by X-ray diffractometer (XRD) and Fourier transform infrared spectroscopy (FT-IR).

## 2. MATERIALS AND METHODS

### 2.1 Materials

The researchers used borogypsum and borax waste provided by the Bandırma Boron Works (Eti Maden, Balıkesir, Turkey). Before starting the experiments, boron waste underwent a preparation process that included drying, grinding, and sieving. The prepared boron waste were identified by XRD and obtained patterns are given in Figure 1. According to XRD results, borogypsum was a mixture of gypsum ( $\text{CaSO}_4 \cdot 2\text{H}_2\text{O}$ , powder diffraction file (pdf) no: 00-006-0046) and calcium borate hydrate ( $\text{Ca}_2\text{B}_{10}\text{O}_{17} \cdot 5\text{H}_2\text{O}$ , pdf no: 00-022-0146) when borax waste was identified as a mixture of dolomite ( $\text{CaMg}(\text{CO}_3)_2$ , pdf no: 01-0073-2361) and tincalconite ( $\text{Na}_2\text{B}_4\text{O}_7 \cdot 5\text{H}_2\text{O}$ , pdf no: 00-007-0277).

Borogypsum-containing mortars were prepared with clinker when borax waste-containing mortars were prepared with CEM 42.5 Portland cement. The binder materials were supplied from Akcansa Cement Factory, Istanbul, Turkey. Because of the gypsum content of borogypsum, clinker was used in the borogypsum-containing mortars.

CEN standard sand conforming to EN 197-1 was supplied by the Limak Trakya Cement (Kırklareli, Turkey) and was used in all mixtures as a fine aggregate. The chemical composition of raw materials was determined by PANalytical MiniPal 4 X-ray

fluorescence (XRF), with parameters ranging from 4 to 30 kV (Table 1).

The nano-CuO used was synthesized from  $\text{CuSO}_4 \cdot 5\text{H}_2\text{O}$  and NaOH by a hydrothermal method. The synthesis reaction temperature and reaction time were set at 70 °C and 4 hours after preliminary experiments with calcination parameters set at 400 °C and 2 hours, respectively. The morphological and crystallographic attributes of nano-CuO were determined by X-ray diffractometry (XRD), scanning electron microscopy (SEM); Micromeritics ASAP 2020 was

TABLE 1. Chemical composition of raw materials

Composition (%)	Clinker	Cement	Borogypsum	Borax waste	Sand
$\text{SiO}_2$	14.00	13.00	4.10	20.00	90.80
$\text{Al}_2\text{O}_3$	3.00	2.00	-	-	5.70
$\text{Fe}_2\text{O}_3$	4.70	4.70	0.99	-	0.86
CaO	76.50	71.80	45.10	57.30	0.41
$\text{SO}_3$	-	2.90	48.70	22.00	-
MgO	-	4.00	-	-	-
$\text{TiO}_2$	-	-	-	-	0.87
$\text{K}_2\text{O}$	1.30	1.20	-	0.95	1.30
$\text{B}_2\text{O}_3$	-	-	1.10	1.30	-
LOI <sup>a</sup>	2.40	2.20	14.50	34.00	2.50

<sup>a</sup>Loss of ignition

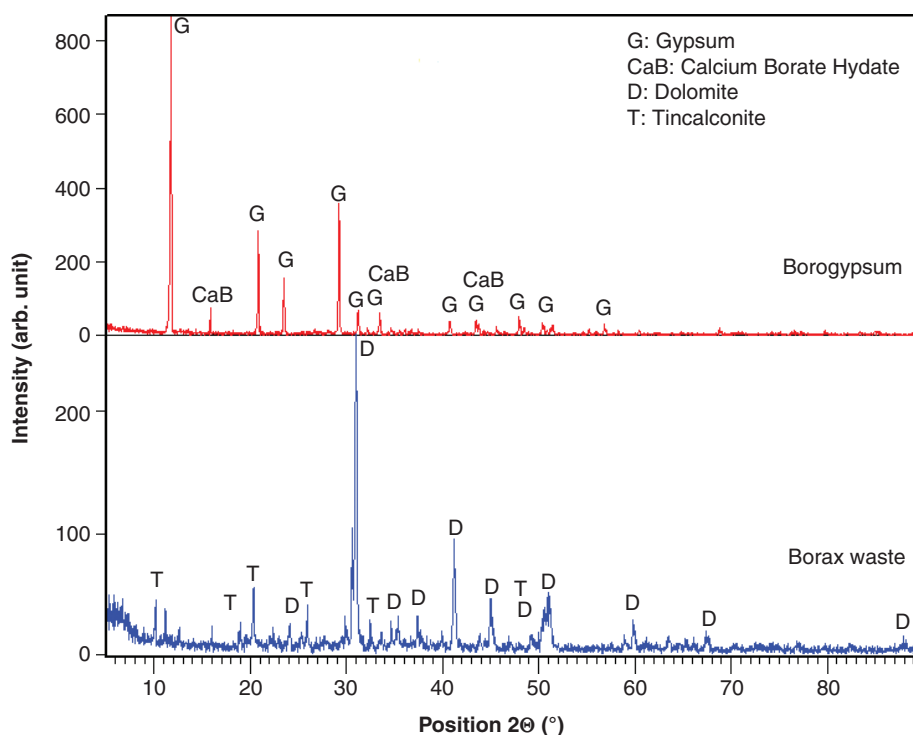


FIGURE 1. XRD patterns of boron wastes.

used to measure the BET-specific surface area ( $S_{\text{BET}}$ ). The XRD pattern of synthesized CuO is presented in Figure 2. Using the XRD results, the product was identified as tenorite (CuO), with a powder diffraction file number (pdf no) 00-045-0937. The Debye-Scherrer equation [Equation 4] was used to calculate the crystallite size of CuO,

$$D=0.94\lambda\beta\cos\Theta \quad [4]$$

where  $D$  is the mean size of crystallites (nm),  $\lambda$  is the X-ray wavelength (1.54 Å),  $B$  is the full width at half maximum (FWHM) and  $\theta$  is the Bragg's angle. The calculation yielded the average size of crystallites as  $24 \pm 6$  nm; this was supported by the SEM image (Figure 3). The  $S_{\text{BET}}$  of nano-CuO was  $45 \text{ m}^2/\text{g}$ .

Because of their large surface area, nanoparticles tend to agglomerate when in contact with water, and dispersing nanoparticles in the mortar matrix can be difficult (8). Thus, MasterGlenium®51, a polycarboxylic ether-based superplasticizer admixture (SP) (BASF Turkey) was used to decrease the attractive forces that cause agglomeration. The technical properties of SP are provided in Table 2.

## 2.2. Mixture proportions

In total, 18 different mixtures with specified amounts of nano-CuO powder were prepared. The amounts of boron waste were kept constant as 3% of binder weight, which was determined as the optimum value according to previous studies (24, 25).

The nanoparticle ratio was varied between 0%–4% of binder. The water to binder ratio of borogypsum and borax waste-containing mixtures were fixed at 0.35 and 0.45, respectively. The chemical composition of boron waste, which led to different water demands of mortars, caused usage of different w/b ratios for each mortar set. The SP ratio used was 0.5% of binder. The detailed mixing proportions of mortars are given in Table 3.

## 2.3. Preparation of specimens

The preparation of specimens was carried out according to the EN 196-1 standard (26), with some changes related to the presence of nano-CuO. To determine a specific preparation method, many preliminary experiments were conducted. In the chosen preparation method, SP was first dissolved in half of the mixing water and nano-CuO was added to this mixture and stirred for 5 minutes at 500 rpm to ensure uniform distribution of the nano-powder. Then, for borogypsum-containing mortars, these components were mixed with borogypsum, clinker and the other half of the water at low speed for 30 seconds, and then within 30 seconds, sand was added to this mixture. For borax waste-containing mortars, the same preparation procedure was carried out by adding borax waste and cement. After stirring for 4 minutes at high speed, the fresh mortars were cast into  $40 \times 40 \times 160$ -mm three-cell prismatic molds. For the water absorption test, the mortar was placed to  $40 \times 40 \times 40$ -mm cubes. The molds were covered with glass plates to avoid

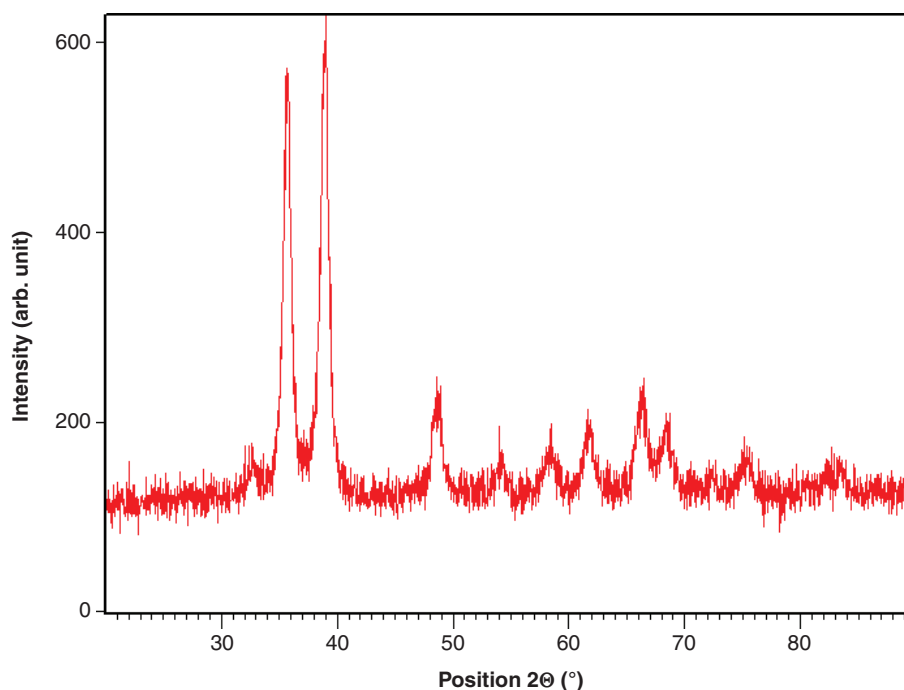


FIGURE 2. XRD pattern of nano-CuO.

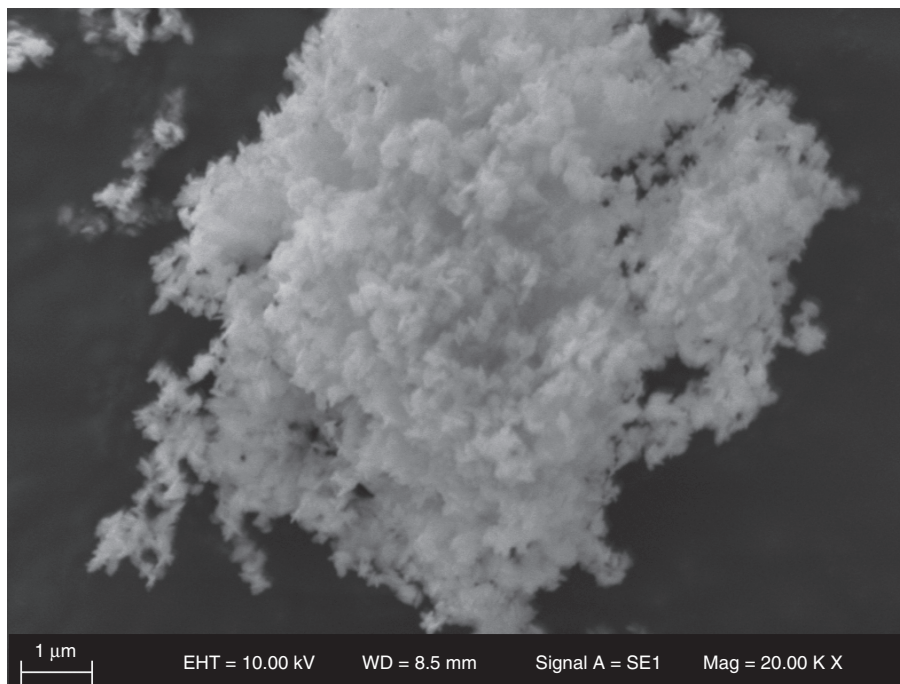


FIGURE 3. SEM image of nano-CuO.

TABLE 2. The technical properties of superplasticizer admixture

Chemical admixture	Composition	Density (kg/L)	Alkaline Content (%) (EN 480-12)	Chloride Content (%) (EN 480-10)
MasterGlenium®51	Polycarboxylic ether	1.082–1.142	< 3	< 0.1

TABLE 3. Mixing proportions of mortar

Mix	Clinker (%)	Cement (%)	BJ (%)	BRX (%)	CuO (%)	Sand (g)	w/b
BJ-C-0	97	-	3	-	0	1350	0.35
BJ-C-1	96.5	-	3	-	0.5	1350	0.35
BJ-C-2	96	-	3	-	1	1350	0.35
BJ-C-3	95.5	-	3	-	1.5	1350	0.35
BJ-C-4	95	-	3	-	2	1350	0.35
BJ-C-5	94.5	-	3	-	2.5	1350	0.35
BJ-C-6	94	-	3	-	3	1350	0.35
BJ-C-7	93.5	-	3	-	3.5	1350	0.35
BJ-C-8	93	-	3	-	4	1350	0.35
BRX-C-0	-	97	-	3	0	1350	0.45
BRX-C-1	-	96.5	-	3	0.5	1350	0.45
BRX-C-2	-	96	-	3	1	1350	0.45
BRX-C-3	-	95.5	-	3	1.5	1350	0.45
BRX-C-4	-	95	-	3	2	1350	0.45
BRX-C-5	-	94.5	-	3	2.5	1350	0.45
BRX-C-6	-	94	-	3	3	1350	0.45
BRX-C-7	-	93.5	-	3	3.5	1350	0.45
BRX-C-8	-	93	-	3	4	1350	0.45

\*BJ: Borogypsum, BRX: Borax waste, C: CuO

water loss because of the heat of hydration and stored in a test cabinet (Nuve TK 120, Turkey) at  $20\pm 2$  °C and 90% relative humidity for 24 hours. Following the demolding, specimens cured in water at a temperature of  $20\pm 2$  °C until the test days.

## 2.4. Test procedure

The setting time of fresh mortar was determined accordance with TS EN 480-2. The effects of different dosages of nano-CuO on the initial and final set time of the mortar were analyzed using a Vicat apparatus through measuring penetration of the metallic needles (27).

Compressive and flexural strength tests were conducted in accordance with EN 196-1 (26) using a UTEST-brand automatic cement compression and flexure testing machine for curing time 3, 7, and 28 days. First, a flexural strength test was carried out, and the two halves obtained were used for a compressive strength test.

The phase analyses of pastes prepared with nano-CuO and boron waste were carried out by XRD in the pattern range of  $5^\circ$  to  $60^\circ$  at a scanning rate of  $0.006^\circ/\text{s}$ . The inorganic crystal structure database (ICSD) patterns were used to identify crystalline composition of pastes. The X-ray tube voltage and current were set at 45 kV and 40 mA, respectively. Fourier transform infrared spectroscopy (FTIR) analysis was conducted in the range  $450$  to  $4000\text{ cm}^{-1}$  to identify characteristic bonding of hydration products. FTIR can determine amorphous phases as well as crystalline phases (28).

The pore structure of mortars was investigated through the BET method. The BET surface areas ( $S_{\text{BET}}$ ) and total pore volume of all samples were determined by nitrogen adsorption on a Micromeritics ASAP 2020 instrument after degassing samples under vacuum at  $105$  °C. Also, to investigate the pore structure, water absorption analysis was conducted at 28 days curing time, in accordance with the BS 1881-122 standard (29). The samples cured for 28 days were dried in the incubator for

72 hours and cooled for 24 hours in a dry airtight vessel after removal from the incubator. The samples were weighed and the mass recorded before immersion in water; the water absorption of the samples was recorded for the immersion periods 10, 30, 60, and 120 min.

Thermal analysis of samples was carried out using PerkinElmer Diamond TG/DTA equipment to measure the heat flow and weight change in the mortars as a function of temperature. Samples that had been cured for 28 days were heated from  $30$  °C to  $1000$  °C at a heating rate of  $10$  °C/min under an  $\text{N}_2$  atmosphere. The amount of CH formation during hydration progress was determined directly by TG analysis from the start and end points of the CH decomposition [5].

$$CH(\%) = WL_{CH}(\%) \times \frac{MW_{CH}}{MW_H} \quad [5]$$

In Equation 5,  $WL_{CH}$  is the weight loss attributable to the CH decomposition,  $MW_{CH}$  and  $MW_H$  are the molecular weights of CH and water, respectively (30).

## 3. RESULTS AND DISCUSSION

### 3.1 Setting time of mortars

The initial and final setting time of mortars prepared with boron waste is shown in Figure 4. In the literature, it has been proven that boron waste retard the hydration process and behave as a set retarder (31). As seen in Figure 4, nano-CuO accelerated hydration, especially in mortars with borax waste at all ratios, reduced the initial and final setting times. Incorporation of 1% nano-CuO made a significant improvement in the final setting time at 38.5% of the control sample, which may be due to the nucleation effect of nano-CuO. On the contrary, the rising ratios of nano-CuO prolonged the final setting time, particularly for borogypsum-containing mortars.

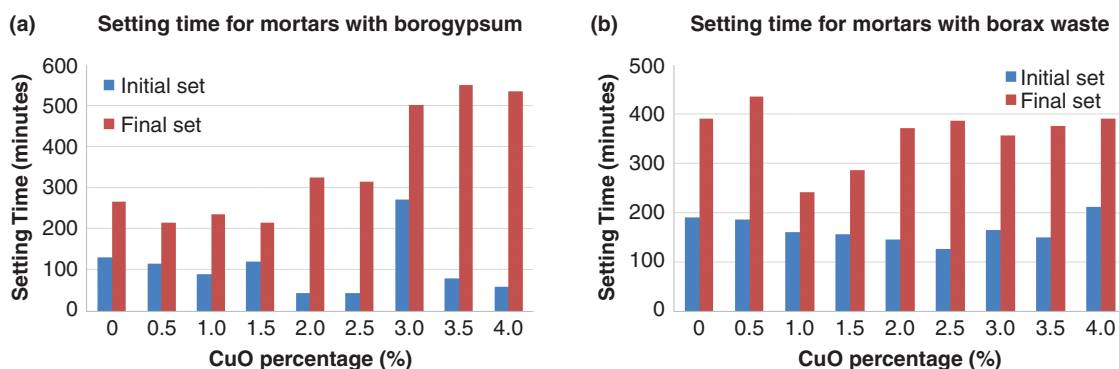


FIGURE 4. Setting time of mortars with a) borogypsum b) borax waste.

### 3.2. Compressive and flexural strength of mortars

The average compressive strength results of mortars containing borogypsum and borax waste for each nano-CuO ratio are presented in Figures 5 and 6, respectively. For all cement mortars, the compressive strength increased with curing time because of continuous hydration and formation of the hydration products C-S-H, C-A-H and C-A-S-H. For mortars including borogypsum, the compressive strength

showed a decrease with the replacement of nano-CuO up to 2%. However, a trend of increase in compressive strength was observed up to 2% nano-CuO addition. The highest compressive strength value was 67.89 MPa after curing 28 days for a 2% nano-CuO addition. Contrarily, for upper nano-CuO ratios, a decrease was observed in the development of compressive strength in comparison with the 2% nano-CuO-containing sample for each number of curing days. The irregular change in compressive strength

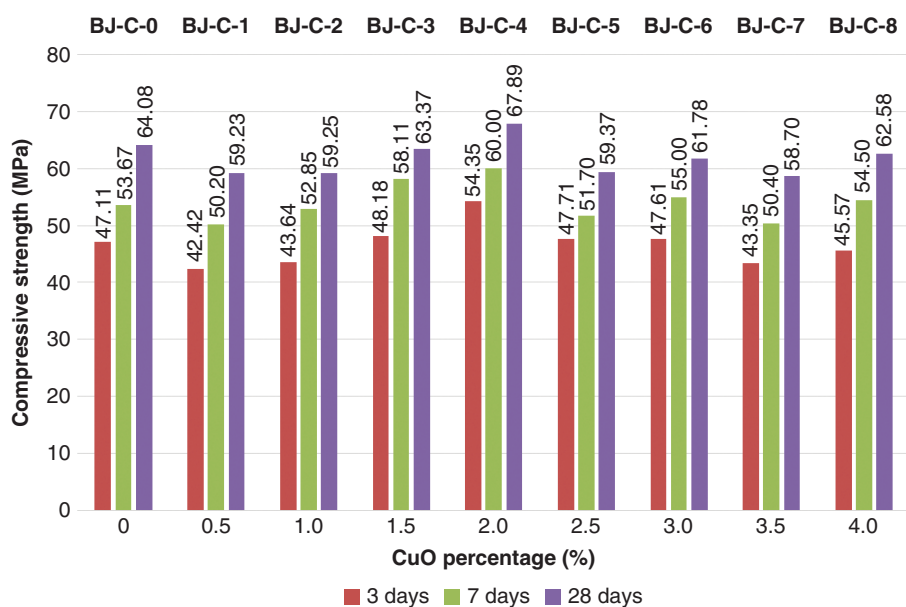


FIGURE 5. Compressive strength of borogypsum containing mortars for different nano-CuO.

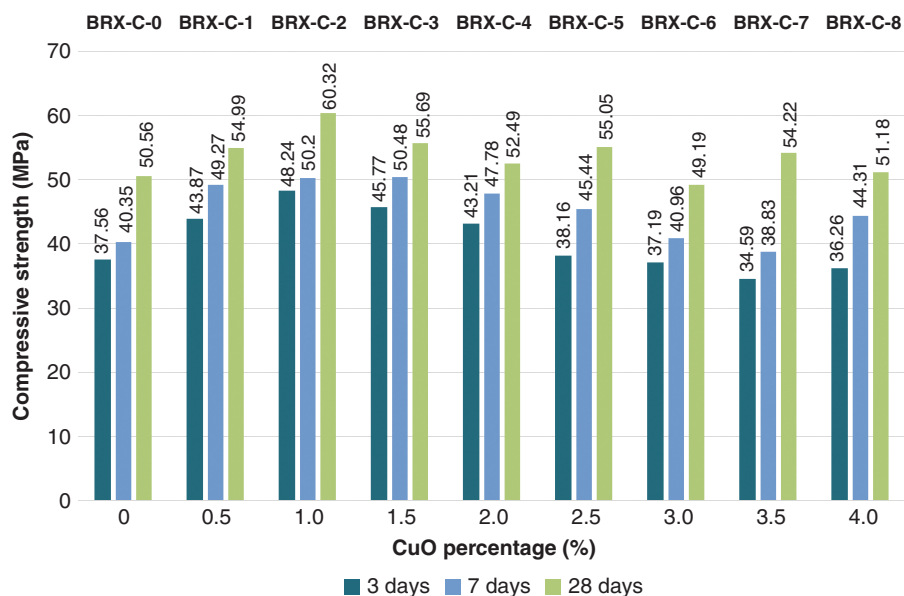


FIGURE 6. Compressive strength of borax waste-containing mortars for different nano-CuO ratios.

by increasing nanoparticle ratios can be explained by different assumptions. Firstly, the reduced amount of binder with increasing amount of nanoparticles lacks the formation and growth of hydration products. Also, acting as foreign nuclei for hydration reactions, the agglomeration of nanoparticles can reduce the surface area of nucleation sites because of dispersion deficiency (10, 18, 32).

In contrast with borogypsum-containing mortars, the reference sample in which borax waste was used showed lower compressive strength as 37.56, 40.35, and 50.56 MPa for curing times of 3, 7, and 28 days, respectively. This phenomenon can be explained by different chemical compositions of boron waste and binders of clinker and cement. Except the sample prepared with 3% CuO, all samples had higher compressive strength than the reference sample. On the other hand, the highest compressive strength value was obtained for 1% nano-CuO replacement as 60.32 MPa for 28 days of curing. When the optimum amount of nano-CuO was added to the mortar matrix, it promoted cement hydration and increased the strength of gel formation. As a result, more hydration products were produced because of the kernel effect of nano-CuO; the compressive strength at 28 days increased up to 24% of the control sample. Similar to studies carried out with nano-CuO (20, 32), the highest compressive strength values were obtained for the range 1% to 3%. In study carried out by Nazari et al. (20), addition of 3% nano-CuO increased the compressive strength of self-compacting concrete with GGBFS as 32% of the reference sample whereas Miyandehi et al. (23) accomplished an

increase in compressive strength value of rice husk ash-containing mortar as 17% of the reference for the same nano-CuO ratio.

The flexural strength results of borogypsum and borax waste-including cement mortars are given in Figures 7 and 8, respectively. Similar to compressive strength, positive influences of nanoparticle addition to cement mortars containing borogypsum were observed only for the samples of BJ-C-4 and BJ-C-5 that contained 2% and 2.5% nano-CuO, respectively. However, even a small amount of nano-CuO (0.5%) produced an improvement of flexural strength to 24.5% of the control sample for borax waste-containing mortars. Nano-CuO behaves like a nano-filler between cement grains and thereby—even not having a pozzolanic effect—the substitution of nano-CuO with cement played a major role in the flexural strength development (11).

### 3.3. XRD results of mortars

Figure 9 illustrates the XRD patterns of samples cured for 28 days. According to XRD analyses, the crystalline composition of the pastes was identified as Portlandite ( $\text{Ca}(\text{OH})_2$ ) with pdf number of 00-044-1481 and Calcium silicate hydrate ( $\text{Ca}_{1.5}\text{SiO}_3 \cdot x\text{H}_2\text{O}$ ) with pdf number of 00-033-0306. When nano-CuO was added to the mortars, the intensity of CH showed a decrease. The reason for this can be the hydration acceleration effect of CuO nanoparticles. For borax waste containing mortars, the highest peak intensity of CSH was observed for BRX-C-3 sample.

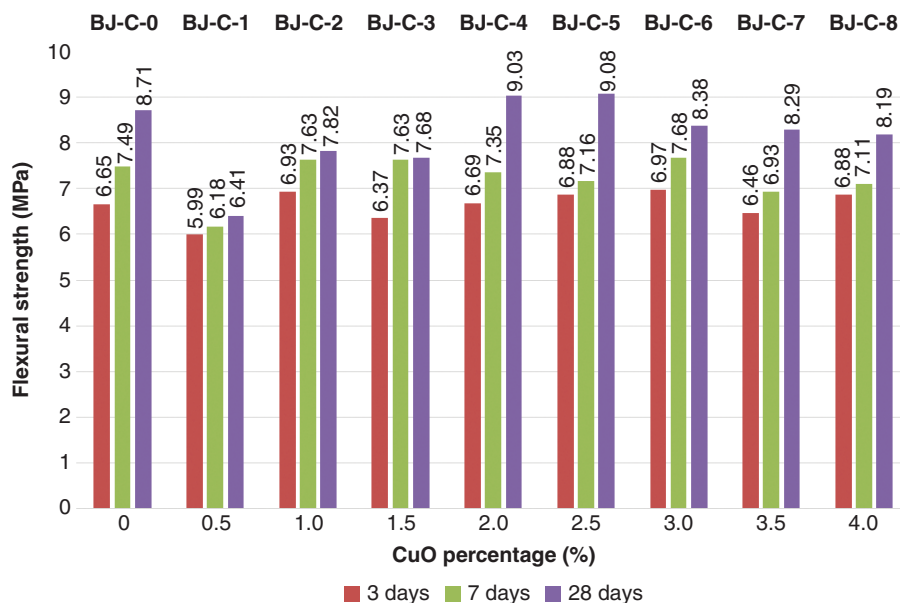


FIGURE 7. Flexural strength of borogypsum containing mortars for different nano-CuO ratios.

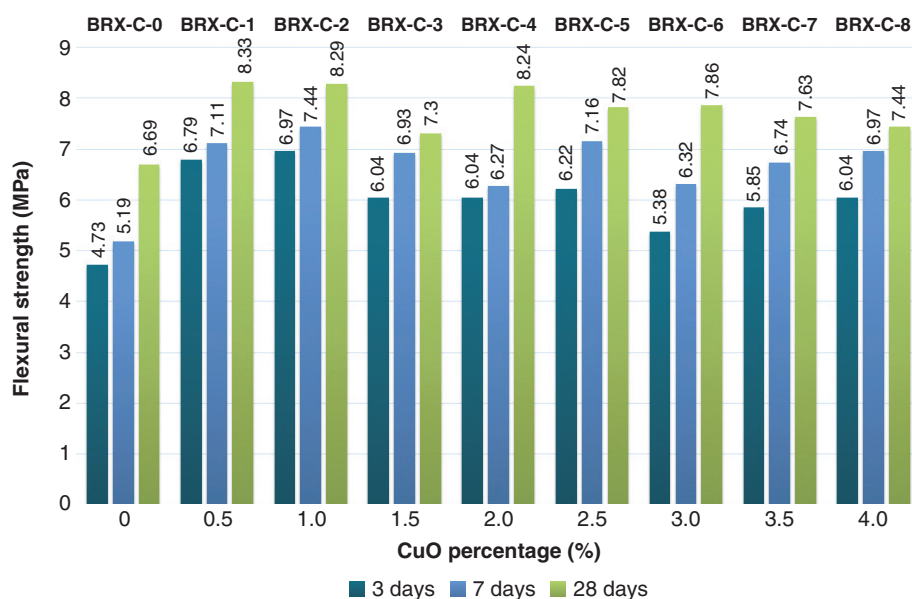


FIGURE 8. Flexural strength of borax waste-containing mortars for different nano-CuO ratios.

### 3.4. FT-IR results of mortars

The FT-IR spectra of mortars prepared with different nano-CuO ratios are given in Figure 10. FT-IR spectra provide information about changes in silicate, sulfate, hydroxide, and carbonate phases during the hydration progress. The IR vibrations between  $3630\text{ cm}^{-1}$  and  $3640\text{ cm}^{-1}$  indicate the non-hydrogen-bonded O-H stretching due to the presence of  $\text{Ca}(\text{OH})_2$ . The peaks between  $2913\text{ cm}^{-1}$  and  $3430\text{ cm}^{-1}$  indicate O-H stretching because of capillary water when the IR absorption bands of O-H bending can be observed around  $1636\text{ cm}^{-1}$ . The peaks that arise around  $1426\text{ cm}^{-1}$  and  $870\text{ cm}^{-1}$  result from carbonization of  $\text{Ca}(\text{OH})_2$  with atmospheric  $\text{CO}_2$ . The peaks between  $1000\text{ cm}^{-1}$  and  $1100\text{ cm}^{-1}$  are due to the silica in the C-S-H gel network, which shows the polymerization of  $\text{SiO}_4^{4-}$ . The peak around  $690\text{ cm}^{-1}$  is accounted for by symmetric bending of Si-O-Si. The out-of-plane Si-O bending causes peaks between  $517\text{ cm}^{-1}$  and  $546\text{ cm}^{-1}$  when the peaks of in-plane Si-O bending are observed around  $464\text{ cm}^{-1}$ . Due to the C-A-S gel, vibration peaks of tetrahedral units of  $\text{AlO}_4$  arise around  $778\text{ cm}^{-1}$  (28, 30, 33–35). In general, the FT-IR spectra of all samples of different nano-CuO compositions showed similarity.

### 3.5. BET analysis results of mortars

The pore volume and specific surface area of cement mortars are given in Table 4. By nitrogen adsorption in BET analysis, properties of the specific surface area and pore volume of samples, which

affect the mechanical and chemical endurance of cement composites, were determined. In BET analysis, the larger specific surface area demonstrates a more compact matrix and smaller pore size (7).

Among the mortars containing borogypsum, all samples had a greater specific surface area compared with the control sample; as a result of this phenomenon, these samples showed a higher total pore volume. When the ratio of nano-CuO increased, a decrease was observed in both specific surface area and total pore volume, which can be caused by the lack of uniform distribution of this nanofiller.

The mortars containing borax waste displayed a significant difference in the values of specific surface area and total pore volume in comparison with mortars with borogypsum. Considering the increasing specific surface area, a more compact mortar matrix was obtained in this experimental set except for the BRX-C-7 sample. In parallel with the results of the strength tests, BRX-C-2 had the highest  $S_{\text{BET}}$ , at  $7.6775\text{ m}^2/\text{g}$ .

To the contrary, although mortars containing borogypsum showed higher compressive and flexural strength, borax waste-containing mortars had a denser structure.

### 3.6. Water absorption results of mortars

The water absorption test results of borogypsum and borax waste-containing mortars are given in Figures 11 and 12, respectively. Figure 10 presents the minimum cumulative water absorption ratio as 0.89% for the BJ-C-4 sample, which also had the highest compressive strength after immersion in

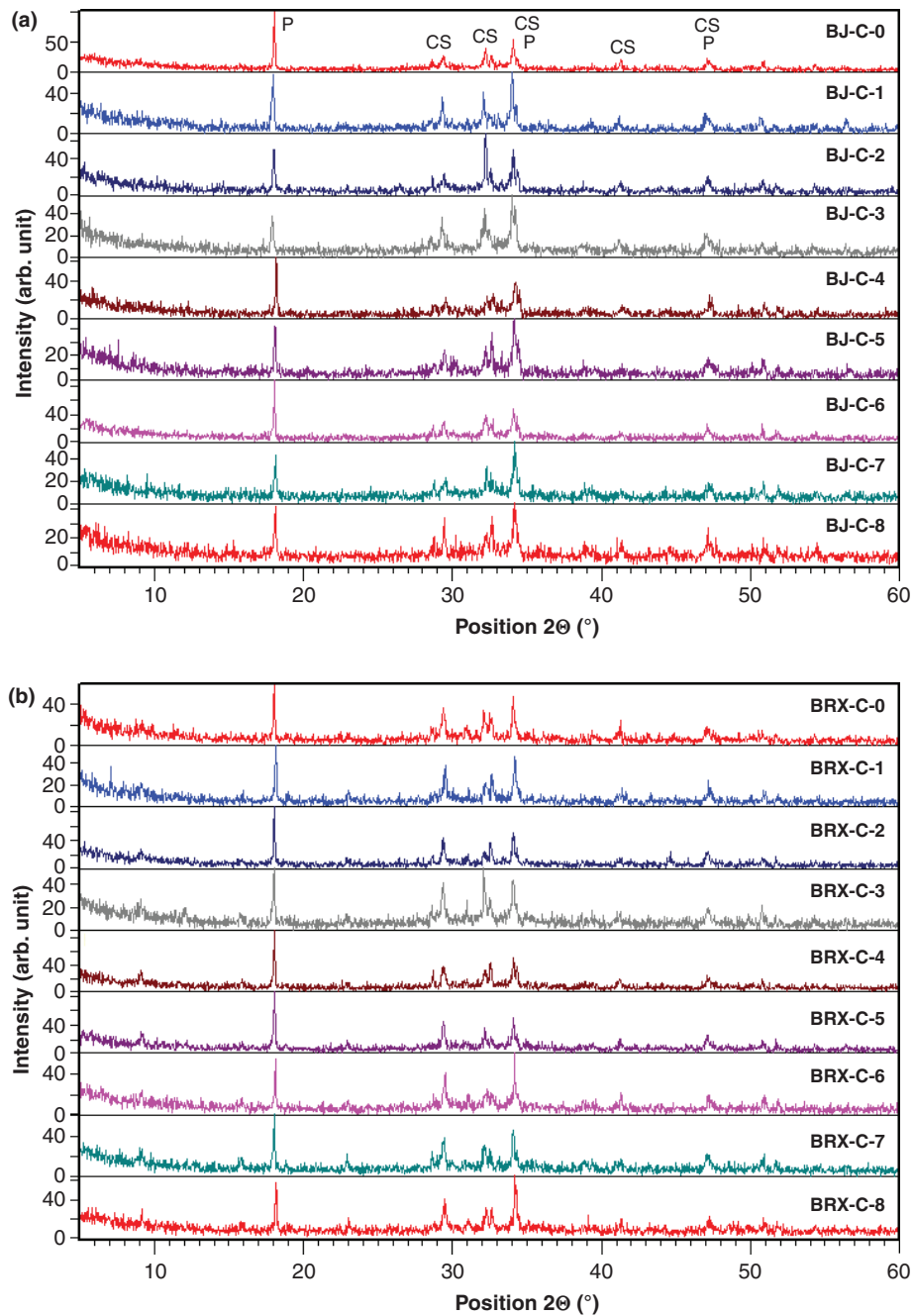


FIGURE 9. XRD patterns of mortars with a) borogypsum and b) borax waste.

water for 120 min. When the reference mix absorbed 3.42% water, increasing nano-CuO above 2.5% caused a similar absorption trend as compared with the reference, whereas the lower ratios reduced the water absorption.

Although the total pore volume of borax waste-containing mortars is greater than the reference mixture indicated by the BET analysis, the water absorption resistance of borax waste-containing mortars was improved by replacement

of nano-CuO. The mortar without nano-CuO absorbed 7.68% water; at 3% nano-CuO, water absorption replacement decreased to 1.41%. The decrease in the water absorption by increasing the amount of nanoparticle can be explained by the reduced porosity.

The comparison of the water absorption results of mortars with different boron waste contents shows that using borogypsum with nanoparticles has a considerable impact on water absorption compared

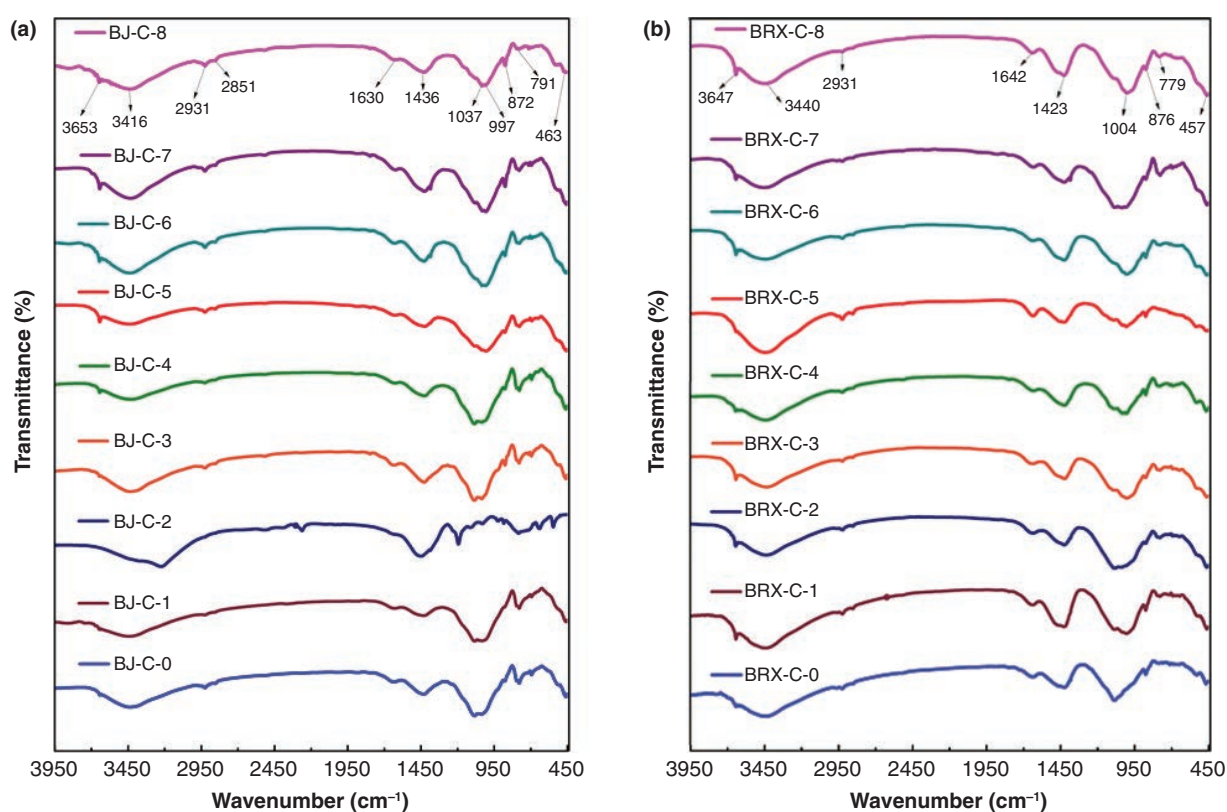


FIGURE 10. FT-IR spectra of mortars with a) borogypsum and b) borax waste for different nano-CuO ratios.

TABLE 4. BET specific area and pore volume of specimens

Mix	$S_{BET}$ (m <sup>2</sup> /g)	Pore Volume (cm <sup>3</sup> /g)
BJ-C-0	1.1739	0.008533
BJ-C-1	4.5244	0.016379
BJ-C-2	4.6515	0.014364
BJ-C-3	3.0636	0.010302
BJ-C-4	3.8215	0.011939
BJ-C-5	2.2284	0.009201
BJ-C-6	1.8825	0.009098
BJ-C-7	1.6418	0.010851
BJ-C-8	1.8759	0.008138
BRX-C-0	3.7321	0.011914
BRX-C-1	4.7800	0.013069
BRX-C-2	7.6775	0.014358
BRX-C-3	6.8768	0.018347
BRX-C-4	6.0937	0.015007
BRX-C-5	3.3164	0.013952
BRX-C-6	3.6724	0.013733
BRX-C-7	1.6714	0.013261
BRX-C-8	3.6879	0.015282

with the borax waste-containing mortars. The water absorption test results conform with compressive and flexural test results in which nano-CuO-modified

borogypsum-containing mortars showed higher strengths than those with addition of borax waste. The higher amount of the C-S-H gel formation in the presence of well-dispersed nano-CuO can ensure a denser packing by filling the space between cement and aggregates, in addition to providing higher mechanical strength.

### 3.7. Thermal analysis results of mortars

Figures 13 and 14 show the differential thermal analysis (DTA) results for mortars containing borogypsum waste and borax waste, respectively. To investigate the effects of nano-CuO replacement on the amount of residual CH in the mortar matrix, analysis results were given in the temperature range 200 °C to 800 °C. Thermal analysis is widely used to estimate amounts of calcium hydrates and CH. TG analysis allows the calculating approximate amount of CH from dehydration between 350 °C and 500 °C, and the decarbonization of CaCO<sub>3</sub> causes mass loss between 600 °C and 800 °C (35–37). In Figures 13 and 14, the decompositions peaks of CH and CaCO<sub>3</sub> were observed for all mixtures. The decomposed amount and the decomposition temperature of CaCO<sub>3</sub> showed similarity for all nano-CuO replacement ratios when the peak temperature of CH decomposition

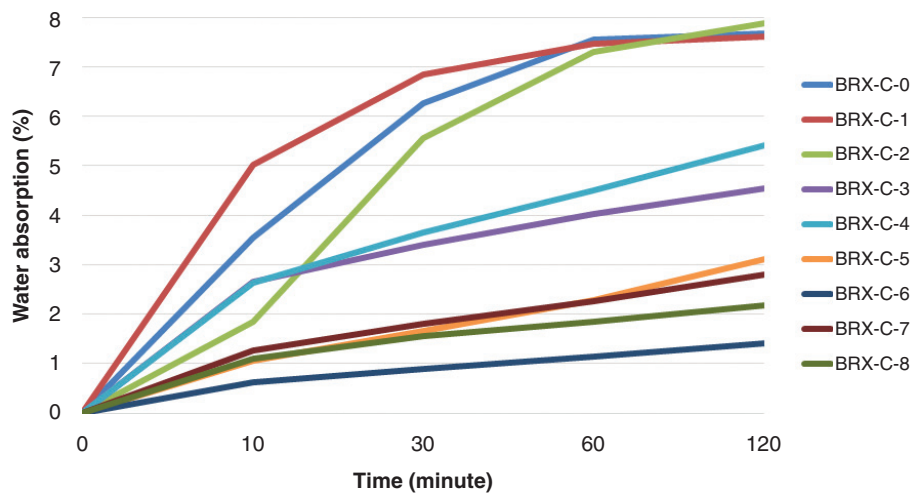


FIGURE 11. Water absorption of borogypsum containing mortars.

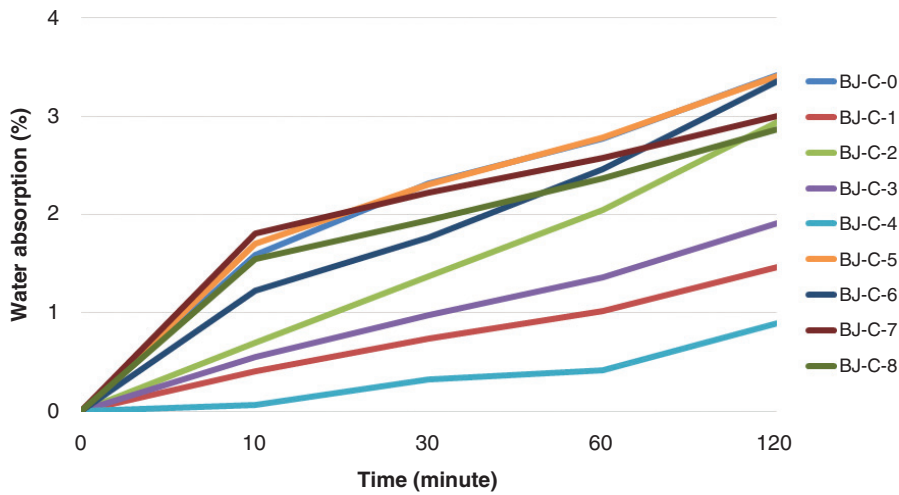


FIGURE 12. Water absorption of borax waste containing mortars.

slightly shifted lower or higher values of reference sample. The decomposition temperature of CH changed between 408.70 °C and 446.89 °C which was in accordance with literature.

Table 5 presents the temperature range of decomposition of CH, the mass loss, % CH content and released heat. According to TG analysis results, when the mass loss because of CH decomposition was 1.09% for the BJ-C-0 sample, the addition of nano-CuO decreased the mass loss percentage for the nano-CuO ratios between 0.5% and 3%. Because the lower CH content indicates more hydration, TG results reveal that using nano-CuO assists further hydration. On the other hand, according to TG analysis, the borax waste-containing composites included more CH than the borogypsum-added mortars, which demonstrates why the BRX-C series had low mechanical strength. The reference

sample BRX-C-0 lost 1.95% of its weight because of decomposition of CH, even though the replacement of nano-CuO up to 1.5% ensured lower amounts of residual CH.

The released heat amount resulting from CH dehydration changed as a function of the amount of decomposed CH. In accordance with mass loss, the incorporation of borax waste into nano-CuO in mortars caused higher released heat resulting from the decomposition of CH.

#### 4. CONCLUSIONS

The researchers in this study examined the effects of nano-CuO on the properties of boron waste (borogypsum and borax waste)-modified cement mortars. Based on the results, the following conclusions can be drawn:

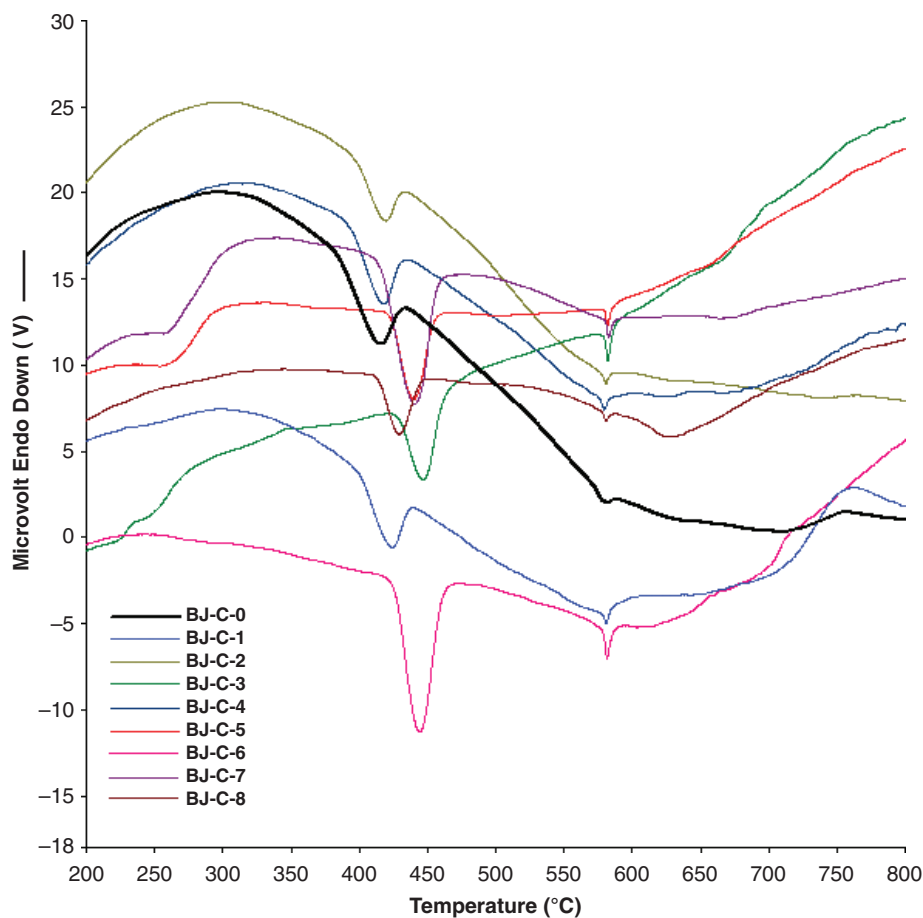


FIGURE 13. DTA results of borogypsum containing mortars.

1. The replacement of CuO accelerated the hydration progress and reduced setting time; even boron-containing waste is known to be materials that have retarding effects on Portland cement hydration. For borax waste-containing mortars, 1% nano-CuO replacement shortened the final setting time by 38.5% compared with the reference sample. Conversely, nano-CuO could not show a positive impact on the setting of borogypsum-added mortars.
2. The addition of 2% nano-CuO provided 67.89 MPa compressive strength after 28 days of curing, which was 6% higher than the reference sample when borogypsum was used. Likewise, the compressive strength increased up to 19.3% of the reference sample for borax waste-containing mortars for 1% nano-CuO addition.
3. BET analysis showed that the pore volume and specific surface area of borogypsum-modified mortars were improved by incorporating nano-CuO at all ratios. However, a non-linear change was observed for the values owing to the non-uniform dispersion of nano-CuO. According to BET results of borax-containing mortars, the combination of borax waste and nano-CuO ensured denser packing.
4. Water absorption results demonstrated that the replacement of nano-CuO was significantly effective in reducing the water absorption of borogypsum-containing mortars, especially for the nano-CuO ratio of 2%. Also, the same effectiveness was observed for borax-containing mortars when the nano-CuO ratio was 3%.
5. The amount of available portlandite (CH) was determined by DTA/TG analysis; addition of nano-CuO in the range 0.5%–3% could decrease the amount of unreacted CH.
6. Experimental results showed different chemical compositions of boron waste enhanced properties to the mortars. Compared to the borax waste, the addition of borogypsum into the mortar composition improved the mechanical properties. Also, BJ-C-0 sample showed 126.53% bigger resistance to the water absorption than BRX-C-0.
7. The results emphasize the significance of choosing the optimal nano-CuO ratio to obtain

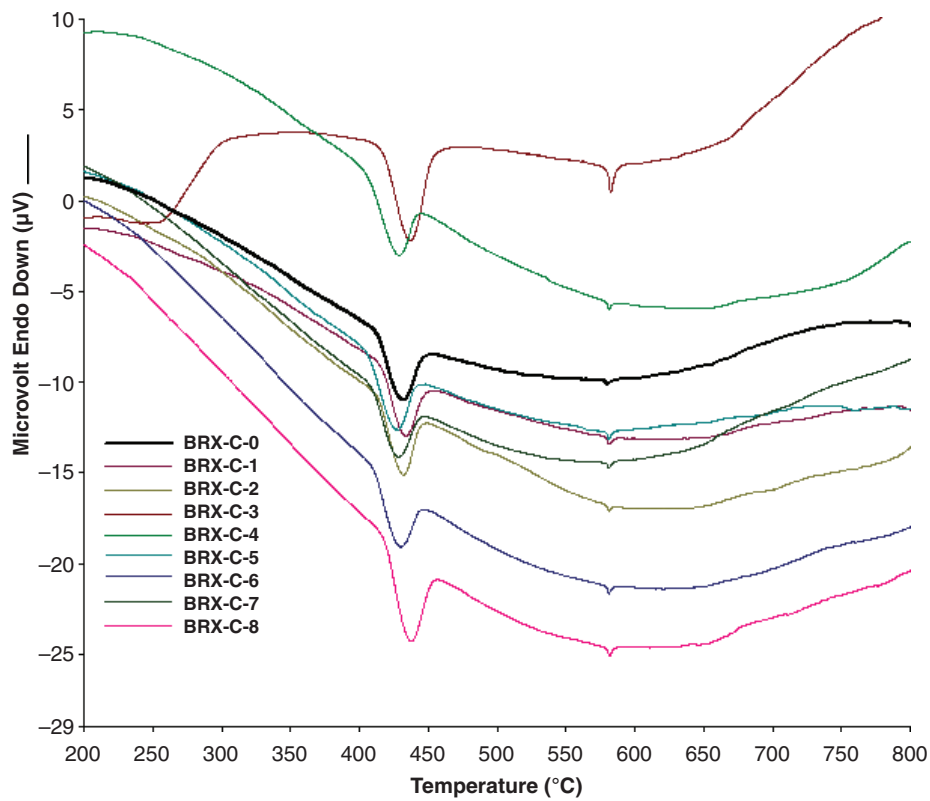


FIGURE 14. DTA results of borax waste containing mortars.

TABLE 5. DTA/TG results of Ca(OH)<sub>2</sub> decomposition

Mix	Initial Temperature (°C)	Final Temperature (°C)	Mass loss (%)	Ca(OH) <sub>2</sub> content (%)	Total heat (kJ/kg)
BJ-C-0	370.78	436.79	1.09	4.48	39.05
BJ-C-1	379.09	458.04	0.83	3.42	34.19
BJ-C-2	379.46	450.72	0.95	3.91	32.55
BJ-C-3	400.50	481.14	0.61	2.51	32.15
BJ-C-4	375.96	446.62	0.85	3.49	30.42
BJ-C-5	401.55	469.92	0.98	4.03	37.35
BJ-C-6	402.40	485.00	1.01	4.15	31.93
BJ-C-7	394.02	491.04	1.62	6.66	37.25
BJ-C-8	398.05	462.00	1.09	4.48	39.23
BRX-C-0	394.78	466.60	1.95	8.02	75.83
BRX-C-1	395.51	461.50	1.36	5.59	47.35
BRX-C-2	395.27	460.99	1.63	6.70	65.17
BRX-C-3	400.89	468.63	0.93	3.82	37.23
BRX-C-4	391.40	456.24	1.79	7.36	75.13
BRX-C-5	387.14	455.28	1.64	6.74	67.27
BRX-C-6	401.31	454.52	1.61	6.62	63.09
BRX-C-7	390.71	456.40	1.99	8.18	80.91
BRX-C-8	401.36	468.31	2.05	8.43	77.97

cement-based composites with desired properties, by reason of the difficulty of the homogeneous distribution of nanoparticles in the composite

matrix. According to obtained results, the appropriate nano-CuO ratio range was determined to be between 2% and 3%.

## ACKNOWLEDGMENTS

This research was supported by Yildiz Technical University Scientific Research Projects Coordination Department, with project number of 2015-07-01-DOP04 and authors wish to extend their sincere thanks to “The Scientific and Technological Research Council of Turkey (TÜBİTAK)” for its Ph.D. scholarship support for the first author.

## References

- Lothenbach, B.; Scrivener, K.; Hooton R.D. (2011) Supplementary cementitious materials. *Cem. Concr. Res.* 41, 1244–1256. <https://doi.org/10.1016/j.cemconres.2010.12.001>.
- Targan, S.; Olgun, A.; Erdogan, Y.; Sevinc, V. (2003) Influence of natural pozzolan, colemanite ore waste, bottom ash, and fly ash on the properties of Portland cement. *Cem. Concr. Res.* 33, 1175–1182. [https://doi.org/10.1016/S0008-8846\(03\)00025-5](https://doi.org/10.1016/S0008-8846(03)00025-5)
- Olgun, A.; Kavas, T.; Erdogan, Y.; Once, G. (2007) Physico-chemical characteristics of chemically activated cement containing boron. *Build. Environ.* 42, 2384–2395. <https://doi.org/10.1016/j.buildenv.2006.06.003>
- Topcu, I.B.; Boga, A.R. (2010) Effect of boron waste on the properties of mortar and concrete. *Waste Manage. Res.* 28, 626–633. <https://doi.org/10.1177/0734242X09345561>
- Banar, M.; Güney, Y.; Özkan, A.; Günkaya, Z.; Bayrakçı, E.; Ulutaş, D. (2016) Utilization of waste clay from boron production in bituminous geosynthetic barrier (GBR-B) production as landfill liner. *Int. J. Polym. Sci.*, Article ID 1648920, <https://doi.org/10.1155/2016/1648920>
- Kula, I.; Olgun, A.; Sevinc, V.; Erdogan Y. (2002) An investigation on the use of tincal ore waste, fly ash, and coal bottom ash as Portland cement replacement materials. *Cem. Concr. Res.* 32, 227–232. [https://doi.org/10.1016/S0008-8846\(01\)00661-5](https://doi.org/10.1016/S0008-8846(01)00661-5)
- Oltulu, M.; Şahin, R. (2014) Pore structure analysis of hardened cement mortars containing silica fume and different nano-powders. *Constr. Build. Mater.* 53, 658–664. <https://doi.org/10.1016/j.conbuildmat.2013.11.105>
- Oltulu, M.; Şahin, R. (2011) Single and combined effects of nano-SiO<sub>2</sub>, nano-Al<sub>2</sub>O<sub>3</sub> and nano-Fe<sub>2</sub>O<sub>3</sub> powders on compressive strength and capillary permeability of cement mortar containing silica fume. *Mat. Sci. Eng. A-Struct.* 528, 7012–7019. <https://doi.org/10.1016/j.msea.2011.05.054>
- Senff, L.; Labrincha, J.A.; Ferreira, V.M.; Hotza, D.; Repette, W.L. (2009) Effect of nano-silica on rheology and fresh properties of cement pastes and mortars. *Constr. Build. Mater.* 23, 2487–2491. <https://doi.org/10.1016/j.conbuildmat.2009.02.005>
- Behfarnia, K.; Salemi, N. (2013) The effects of nano-silica and nano-alumina on frost resistance of normal concrete. *Constr. Build. Mater.* 48, 580–584. <https://doi.org/10.1016/j.conbuildmat.2013.07.088>
- Oltulu, M.; Şahin, R. (2013) Effect of nano-SiO<sub>2</sub>, nano-Al<sub>2</sub>O<sub>3</sub> and nano-Fe<sub>2</sub>O<sub>3</sub> powders on compressive strengths and capillary water absorption of cement mortar containing fly ash: A comparative study. *Energy Buildings*, 58, 292–301. <https://doi.org/10.1016/j.enbuild.2012.12.014>
- Heikal, M.; Ismail, M.N.; Ibrahim, N.S. (2015) Physico-mechanical, microstructure characteristics and fire resistance of cement pastes containing Al<sub>2</sub>O<sub>3</sub> nano-particles. *Constr. Build. Mater.* 91, 232–242. <https://doi.org/10.1016/j.conbuildmat.2015.05.036>
- Yu, R.; Spiesz, P.; Brouwers, H.J.H.; (2014) Effect of nano-silica on the hydration and microstructure development of Ultra-High Performance Concrete (UHPC) with a low binder amount. *Constr. Build. Mater.* 65, 140–150. <https://doi.org/10.1016/j.conbuildmat.2014.04.063>
- Farzadnia, N.; Abang Ali, A.A.; Demirboga R.; (2013) Characterization of high strength mortars with nano alumina at elevated temperatures. *Cem. Concr. Res.* 54, 43–54. <https://doi.org/10.1016/j.cemconres.2013.08.003>
- Jalal, M.; Fathi, M.; Farzad, M.; (2013) Effects of fly ash and TiO<sub>2</sub> nanoparticles on rheological, mechanical, micro-structural and thermal properties of high strength self-compacting concrete. *Mech. Mater.* 61, 11–27. <https://doi.org/10.1016/j.mechmat.2013.01.010>
- Arefi, M.R.; Rezaei-Zarchi, S. (2012) Synthesis of zinc oxide nanoparticles and their effect on the compressive strength and setting time of self-compacted concrete paste as cementitious composites. *Int. J. Mol. Sci.*, 13, 4340–4350. <https://doi.org/10.3390/ijms13044340>
- Qing, Y.; Zenan, Z.; Deyu, K.; Rongshen, C. (2007) Influence of nano-SiO<sub>2</sub> addition on properties of hardened cement paste as compared with silica fume. *Constr. Build. Mater.* 21, 539–545. <https://doi.org/10.1016/j.conbuildmat.2005.09.001>
- Li, Z.; Wang, H.; He, S.; Lu, Y.; Wang, M. (2006). Investigations on the preparation and mechanical properties of the nano-alumina reinforced cement composite. *Mater. Lett.* 60, 356–359. <https://doi.org/10.1016/j.matlet.2005.08.061>
- Said, A.M.; Zeidan, M.S.; Bassuoni, M.T.; Tian, Y. (2012) Properties of concrete incorporating nano-silica. *Constr. Build. Mater.* 36, 838–844. <https://doi.org/10.1016/j.conbuildmat.2012.06.044>
- Nazari, A.; Riahi, S. (2011) Effects of CuO nanoparticles on compressive strength of self-compacting concrete, *Sādhanā*, 36, 371–391. <https://doi.org/10.1007/s12046-011-0023-7>
- Nazari, A.; Riahi, S. (2011) Effects of CuO Nanoparticles on microstructure, physical, mechanical and thermal properties of self-compacting cementitious composites. *J. Mater. Sci. Technol.* 27, 81–92. [https://doi.org/10.1016/S1005-0302\(11\)60030-3](https://doi.org/10.1016/S1005-0302(11)60030-3)
- Nazari, A.; Rafieipour, M. H.; Riahi, S. (2011) The effects of CuO nanoparticles on properties of self compacting concrete with GGBFS as binder. *Mater. Res.* 14 [3], 307–316. <https://doi.org/10.1590/S1516-14392011005000061>
- Miyandehi, B.M.; Feizbakhsh, A.; Yazdi, M.A.; Liu, Q.; Yang, J.; Alipour, P. (2016) Performance and properties of mortar mixed with nano-CuO and rice husk ash. *Cem. Conc. Comp.* 74, 225–235. <https://doi.org/10.1016/j.cemconcomp.2016.10.006>
- Ozdemir, M.; Uygan Ozturk, N. (2003) Utilization of clay wastes containing boron as cement additives. *Cem. Concr. Res.* 33, 1659–1661. [https://doi.org/10.1016/S0008-8846\(03\)00138-8](https://doi.org/10.1016/S0008-8846(03)00138-8)
- Kula, I.; Olgun, A.; Erdogan, Y.; Sevinc, V. (2001) Effects of colemanite waste, coal bottom ash, and fly ash on the properties of cement. *Cem. Concr. Res.* 31, 491–494. [https://doi.org/10.1016/S0008-8846\(00\)00486-5](https://doi.org/10.1016/S0008-8846(00)00486-5)
- TS EN 196-1 (2009) Methods of testing cement - Part 1: Determination of strength.
- TS EN 480-2 (2008) Admixtures for concrete, mortar and grout - Test methods - Part 2: Determination of setting time.
- Holley, J. C.; Paine, K.; Papatzani, S. (2014) Effects of nano-silica on the calcium silicate hydrates in Portland cement-fly ash systems. *Adv. Cem. Res.* <https://doi.org/10.1680/acr.13.00098>
- BS 1881-122 (2011) Testing concrete: Method for determination of water absorption.
- Singh, L.P.; Agarwal, S.K.; Bhattacharyya, S.K.; Sharma, U.; Ahalawat, S.; (2011) Preparation of silica nanoparticles and its beneficial role in cementitious materials. *Nanomater. Nanotechnol.* 1, 44–51. <https://doi.org/10.5772/50950>
- Erdogan, Y.; Zeybek, M.S.; Demirbaş, A. (1998) Cement mixes containing colemanite from concentrator wastes. *Cem. Concr. Res.* 28, 605–609. [https://doi.org/10.1016/S0008-8846\(98\)00018-0](https://doi.org/10.1016/S0008-8846(98)00018-0)
- Khotbehsara, M.M.; Mohseni, E.; Yazdi, M.A.; Sarker, P.; Ranjbar, M.M. (2015) Effect of nano-CuO and fly ash on the properties of self-compacting mortar. *Constr. Build. Mater.* 94, 758–766. <https://doi.org/10.1016/j.conbuildmat.2015.07.063>
- Choudhary, H.K.; Anupama, A.V.; Kumar, R.; Panzi, M.E.; Matteppanavar, S.; Sherikar, B.N.; Sahoo, B. (2015) Observation of phase transformations in cement during

- hydration. *Constr. Build. Mater.* 101, 122–129. <https://doi.org/10.1016/j.conbuildmat.2015.10.027>
34. Ghosh, S.N. (2002) IR spectroscopy: First edition in Handbook of analytical techniques in concrete science and technology, William Andrew Publishing, New York, (2002).
35. Barbhuiya, S.; Mukherjee, S.; Nikraz, H. (2014). Effects of nano- $\text{Al}_2\text{O}_3$  on early-age microstructural properties of cement paste. *Constr. Build. Mater.* 52, 189–193. <https://doi.org/10.1016/j.conbuildmat.2013.11.010>
36. Vedalakshmi, R.; Sundara, Raj, A.; Palaniswamy, N. (2008) Identification of various chemical phenomena in concrete using thermal analysis. *Indian J. Chem. Sect A*, 15, 388–396.
37. Ramachandran, V.S.; Paroli, R.M.; Beaudoin, J.J.; Delgado, A.H. (2002) Handbook of thermal analysis of construction materials, Noyes Publications, New York, (2002).